



Characterization of spontaneous seizures and EEG abnormalities in a mouse model of the human A350V IQSEC2 mutation and identification of a possible target for precision medicine based therapy

Owen Kane^{a,1}, Almedia McCoy^{a,1}, Reem Jada^c, Veronika Borisov^c, Liron Zag^c, Amir Zag^c, Kinneret Schragenheim-Rozales^c, Reut Shalgi^c, Nina S. Levy^c, Andrew P. Levy^{c,*}, Eric D. Marsh^{a,b,*}

^a Division of Neurology, Children's Hospital of Philadelphia, Philadelphia, PA, USA

^b Departments of Neurology and Pediatrics, University of Pennsylvania Perelman School of Medicine, Philadelphia, PA, USA

^c Technion Faculty of Medicine, Technion-Israel Institute of Technology, Haifa, Israel

ARTICLE INFO

Keywords:

IQSEC2
Seizures
TRH
Delta waves
EEG

ABSTRACT

IQSEC2 is an X-linked gene localized to the post synaptic density encoding a GTP exchange factor that regulates NMDA mediated changes in synaptic function. Mutations in the IQSEC2 gene are associated with drug resistant epilepsy, intellectual disability and autism. Precision medicine based therapeutics to treat IQSEC2 associated epilepsy requires the development and characterization of mutation specific animal models. To date no EEG recordings have been presented for any mouse model of any IQSEC2 mutation showing seizures. In this study we characterize the seizures and EEG brain wave abnormalities present in mice with a A350V IQSEC2 missense mutation that is associated with drug resistant epilepsy in man. We show that seizures are associated with a greater than 40% mortality rate in male mice and occur exclusively from post-natal day 16–20. EEG recordings of mouse pups during this window demonstrate seizures and the presence of spikes with a marked increase in delta waves. EEG recordings in adult male mice have persistent excessive slow frequency activity and spikes, but seizures were not recorded. RNAseq analysis of the hippocampi of mice prior to the development of seizures demonstrated marked abnormalities in canonical pathways involved in synaptogenesis and dendritic maturation with the most prominently dysregulated gene being that for TRH suggesting a potential target for therapy given the previous demonstration of TRH to decrease seizures in several forms of drug resistant epilepsy.

1. Introduction

Mutations in the human IQSEC2 gene (NM_001111125) (MIM 300522) on chromosome Xp11.22 have been associated with severe intellectual disability, epilepsy and autism like features (Shoubbridge et al., 2010b, 2019; Zerem et al., 2016; Mignot and Depienne, 2019). Seizures in male children with IQSEC2 mutations have been reported to be drug resistant in over 80% of cases (Mignot and Depienne, 2019).

Accordingly, the development of animal models of IQSEC2 mutation induced epilepsy would be of considerable value in developing precision medicine based therapies to reduce seizure burden. Towards this goal in this study we characterize the seizures present in mice with a A350V IQSEC2 missense mutation that is associated with drug resistant epilepsy in human (Zipper et al., 2017).

The mouse IQSEC2 gene (NM_001005475) is over 98.5% homologous to the human IQSEC2 gene with complete conservation of all

Abbreviations: qRT-PCR, quantitative reverse transcriptase polymerase chain reaction; DEG, differentially expressed genes; EEG, electroencephalography; TRH, Thyrotropin Releasing Hormone; RNAseq, RNA sequencing.

* Corresponding author.

* Corresponding author at: Division of Neurology, Children's Hospital of Philadelphia, Philadelphia, PA, USA.

E-mail addresses: OWK2@pitt.edu (O. Kane), mccoya@chop.edu (A. McCoy), reemjada@campus.technion.ac.il (R. Jada), veronikabor@campus.technion.ac.il (V. Borisov), lironz@campus.technion.ac.il (L. Zag), azangi@alumni.technion.ac.il (A. Zag), kinnere9@campus.technion.ac.il (K. Schragenheim-Rozales), reutshalgi@technion.ac.il (R. Shalgi), ninal@technion.ac.il (N.S. Levy), alevy@technion.ac.il (A.P. Levy), marshe@chop.edu (E.D. Marsh).

¹ These authors contributed equally to this work.

<https://doi.org/10.1016/j.epilepsyres.2022.106907>

Received 29 July 2021; Received in revised form 1 February 2022; Accepted 11 March 2022

Available online 15 March 2022

0920-1211/© 2022 Elsevier B.V. All rights reserved.

functional domains. We recently reported on the creation of A350V IQSEC2 mice and abnormalities in their social behavior and cognition (Rogers et al., 2019). Initial characterization of the A350V IQSEC2 mice revealed that seizures were frequently visually observed in young pups (P16–P20) (Levy et al., 2019), but we did not record EEGs at this age or in the adult ages. While performing EEGs in mice of this age are technically challenging, studies have been successful in performing EEGs at this young age and capturing seizures (Marsh et al., 2009; Scantlebury et al., 2010a; Raol et al., 2009). Confirming visually detected seizures and quantifying EEG changes we report here on the characterization by EEG of the brain wave abnormalities, spikes and seizures in pups and adults with the A350V IQSEC2 mutation.

IQSEC2 is located at the post synaptic density of both excitatory neurons and parvalbumin interneurons (Murphy et al., 2006; Sah, 2020). IQSEC2 functions as a GTP exchange factor (GEF) for ARF6 thereby regulating dendritic spine morphogenesis (Hinze et al., 2017) and membrane trafficking of AMPA receptors (Myers et al., 2012; Brown et al., 2016). IQSEC2 is regulated by calcium via the interaction of calmodulin with a IQ domain (IQ SEC2 amino acid residues 357–370) in the IQSEC2 gene and dysregulation of this regulatory mechanism is thought to mediate the pathophysiology underlying the A350V IQSEC2 mutation via constitutively activating the GEF activity of IQSEC2 (Rogers et al., 2019). However, the mechanism of how the A350V mutation results in seizures is not known. Therefore, we performed RNAseq on Post-natal day (P)16 mice followed by bioinformatics analysis in order to identify potential pathways and networks that might provide insights and targets for therapy.

2. Methods

2.1. Mice used in this study

The creation of A350V IQSEC2 mice in a C57/Bl6J background was previously described as well as the PCR based genotyping strategy used to distinguish the mutant allele from the wild type allele (Rogers 2019). Mice were housed and maintained both at the Technion Faculty of Medicine as well as at the Children's Hospital of Philadelphia germ free animal facility per under the approval of the respective institutional animal care and use committees (IL1691117 at Technion and 622 at Children's Hospital of Philadelphia (CHOP)). Mice were permitted unlimited access to food and water during these studies.

2.2. Seizures and survival

For each litter born the number of animals that died at a given age were calculated. To compared survival across groups a Kaplan-Meier survival curve was generated and the survival between genotypes and locations was compared by log-rank. Pups between P10–P21 were video recorded and tracked using Datawave video bench software. The video was reviewed by one reviewer (OK) who looked for events of backing up, head bobbing, tail stiffening, rapid grooming movements (and these movements in a sequence), and “popcorn” movements (when the animal bounced around the cage). These movements approximate the stages of seizures (Michalakakis et al., 1998).

2.3. EEG recordings

Video EEGs were performed as previously described (Marsh, 2009; Ahrens-Nicklas et al., 2019). Mice were housed in a temperature-controlled environment with a fixed day-night schedule with unlimited access to food and water. Three groups of animals were studied. Pups at P14–P21 were recorded for 2–4 h at a stretch and returned to dams. IQSEC2 mutant mice and littermate controls who survived past P21 were recorded between P30 and P90 for 72 h to determine if seizures were present in adult animals.

For EEG, the mice were implanted with electrodes under isoflurane

anesthesia with local application of lidocaine for analgesia. In adult animals, electrodes were placed under stereotaxic placement (all coordinates from Bregma) of 8 electrodes (bifrontal cortex (0.5 mm Anterior–Posterior [A–P], 1.0 mm medial–lateral [M–L]), bilateral visual area (–3.5 Anterior–Posterior [A–P], 2 mm medial lateral [M–L]), bilateral parietal (–0.7 A–P, 3 mm M–L), and bilateral hippocampal depth (–2.2 mm A–P, 2.0 mm M–L and 1.7 mm ventral). For these animals, screws (#000 Small Parts Co.) were placed in the frontal and occipital locations and a 0.005 in. silver wire (125 μ m; A-M systems, Carlsborg, WA) were placed in the dorsal hippocampus. The wires were attached to an Omnetics nano 16-Pin connector (Omnetics corporation). Ground and reference electrodes were placed on either side of the midline directly behind the Lambda suture. For P14–21 animals, a screw (#000 Small Parts Co.) was placed in the midline in front of Bregma and used as ground and another screw placed behind Lambda suture and used as reference. 8 electrodes were placed 1 mm on either side of the midline at 1.5, 3, 4.5 and 6 mm behind Bregma. The wires were placed at the level of the cortical surface. For animals over P30, the mice were then allowed to recover for 24–48 h in their home cage before transferring to the recording cage for 72 h. The animals were recorded for 72 h and then returned to the home cage and then re-recorded weekly to P90. For the P15–P21 mice, after implant they were returned to the dam to recover for 24 h and then recorded for 2–4 h twice in a day and returned to the dam and recorded for 2–6 days as tolerated. At any sign of discomfort, weight loss, or injury the pups were euthanized. For all mice, the EEG was record at a 1000 Hz sampling rate on a Intan Extracellular recording system (Intan Technologies) and viewed using on-line low-pass (100 Hz) and high-pass (0.5 Hz) filters with a 60 Hz notch filter in place.

For analysis, the video EEGs were reviewed for the presence of seizures. The frequency of the background EEG was quantified by measuring the entire EEG recording in 5 s segments. For each segment, a Fast Fourier Transform (FFT) was calculated (MATLAB 2010b, Mathworks, Inc., Natick, MA) and the power in selected bandwidths (Delta 0.1–3.5 Hz, Theta 3.5–8.5 Hz, Alpha 8.5–13 Hz, Beta 13–25 Hz, and Gamma 25–100 Hz) determined using a TrapZ function in Matlab. The resultant power bands were normalized by dividing by total FFT power (0.5–200 Hz). Light on and light off times were analyzed separately and then the entire recording analyzed. To clean the EEG prior to performing FFT calculations the EEG was run through an in-house algorithm that performs EEG artifact detection. For EEG artifact rejection, the root mean squared amplitude and skew was calculated and a channel with an RMS > 200 or < 30 and skew > 0.4 rejected outright. The RMS and skew cut offs were generated by measuring these values in a normal EEG and then choosing thresholds that are only observed in artifact channels. After the channel-based analysis, an RMS z-score will be generated for each 5 s segment and then the segment FFT not analyzed if the z-score is > 3. This method allows a completely unbiased analysis of the background EEG (Ahrens-Nicklas et al., 2019; Yun 2018). In order to compare genotypes and frequencies over time, a 2 way ANOVA with post-hoc multiple comparisons using Sidák's multiple comparisons test (Prism software, Graph Pad, San Diego USA) was used determine statistically significant differences. P values for genotype x frequency and then for multiple comparisons are presented.

2.4. RNAseq and analysis

RNAseq and analysis was performed at the Genomics Center of the Biomedical Core Facility (BCF) of the Technion Faculty of Medicine. This analysis was performed on RNA obtained from the hippocampi of 4 male A350V IQSEC2 mutant and three male IQSEC2 wild type mice from the same litter from a mating between a female heterozygous for the A350V IQSEC2 mutation and a wild type IQSEC2 male. The reason we chose to focus on the hippocampus for this analysis is that (1) within the brain the expression of IQSEC2 is highest in the hippocampus (Sakagami et al., 2008) and (2) all prior work assessing the function of IQSEC2 has

been done in hippocampal cultures (Hinze et al., 2017; Brown JC et al., 2016).

Total RNA was extracted from these seven mouse hippocampus tissue samples after homogenization using the Qiacube (Qiagen). Seven RNAseq libraries were constructed simultaneously according to the manufacturer's protocol (NEBNext Ultra II Directional RNA Library Prep Kit for Illumina, cat no. E7760) using 800 ng total RNA as starting material. The RNAseq data was generated on Illumina NextSeq500, 75 cycles (single read), high-output mode (Illumina, cat no. 20024906). Quality control was assessed using Fastqc (v0.11.5), reads were trimmed for adapters, low quality 3' and minimum length of 20 using CUTADAPT (v1.12). 84 bp single-end reads were aligned to the Mouse reference genome (Mus_musculus.GRCm38.dna.primary_assembly.fa from ENSEMBL) and annotation file (Mus_musculus.GRCm38.92.gtf from ENSEMBL) using STAR aligner (v2.6.0a). The number of reads per gene was counted using Htseq-count (v0.9.1). A statistical analysis was performed using DESeq2 R package (version 1.20.0) (Genome Biology 2014 15:550). The number of reads per gene was extracted into Count.xls and NormalizedCounts.xls files for raw counts and normalized counts, respectively. Results of the statistical analysis, i.e. list of the differentially expressed genes (DEGs) is provided as on line supplement #1 with the p value (corrected for multiple comparisons to reduce the false discovery rate) and fold change in each gene shown (DESeq2_results.xls). The 431 DEGs were analyzed using the Qiagen ingenuity pathway analysis software for canonical pathways, networks and diseases in order to identify those pathways which were significantly affected by the A350V mutation and in which specific neurological diseases were associated with these DEGs.

2.5. qRT-PCR for TRH

Quantitative real time-polymerase chain reaction (qRT-PCR) was performed from 6 A350V IQSEC2 and 6 WT IQSEC2 hippocampal RNA at d16 from three different litters of mice. RNA was isolated using RNAeasy mini kit (Qiagen). RNA was converted to cDNA using the high capacity cDNA reverse transcriptase kit with RNase inhibitor (Applied Biosystems AB4374966) and qRT-PCR was performed with Fast SYBR Green master mix (Applied Biosystems AB-4385612) using the StepOnePlus Real-Time PCR system (ThermoFisher 4376600). Signals for TRH were normalized to the housekeeping gene HPRT.

RT-PCR primers: TRH (F) GATTCTGGAGCCTTGCAGAC & (R) GGGGATACCAAGTTAGACGA; HPRT F: CAGTCCAGCGTCGTGATTA & R: TGGCCTCCCATCTCCTTCAT.

3. Results

3.1. Increased mortality after seizures in A350V IQSEC2 mice

In our initial characterization of male and female mice (heterozygote and homozygous for the A350V mutation) we observed frequent seizures manifested as irregular clonic movements with involuntary and uncontrolled movements often associated with the mouse falling on its side and exhibiting tonic clonic movements of all extremities. Nearly all mice viewed to have these seizures died within 1–2 h. All visualized seizures were observed between days 15–20 after birth. The mortality of mice in the Technion colony are shown in Fig. 1a demonstrating a greater than 40% mortality rate in male mice hemizygous for the A350V period and approximately half that rate in female mice heterozygous for the A350V mutation consistent with the random X inactivation of the IQSEC2 gene in mice. This increased mortality rate in the male mice was observed regardless of whether the mother of the pups was heterozygous or homozygous for the A350V IQSEC2 mutation. The mortality rate in females homozygous for the A350V mutation was similar to that seen in males hemizygous for the mutation. A Kaplan Meir survival curve (Fig. 1b) demonstrates that the peak day of death in the male hemizygous mice was between d17–18 with 50% of the deaths occurring between these two days. No mortality was observed in any A350V mice (female or male) after d21 up to 8 months of age when the A350V mice were sacrificed. An identical mortality (frequency and time course) was found in the A350V IQSEC2 colony at the Technion and at CHOP (Fig. 1b).

3.2. Characterization of seizures, spikes and brain waves on EEG

Pups were video recorded for 2–4 h, once or twice a day to capture and quantify seizure like movements. Analysis of video from 27 pups (n = 12 WT IQSEC2^{X/Y} males, 10 mutant hemizygous IQSEC2^{A350V/Y} males) and 5 homozygous IQSEC2^{A350V/A350V} females and 2 heterozygous IQSEC2^{A350V/X} females) over 11 days (P10–P21) with 419.25 total hours (range per mouse 2–23.5; 17.5 median hours; range on any day 3.5–56.5; 32.125 median hours) revealed that 3 of 10 male mutant pups had seizures and 2 of 5 homozygous mutant females had seizures. We observed 10 seizures in these 5 mice demonstrating stage 5 seizures (popcorn seizures). These were observed in the knockout males and homozygous females (see video supplements 1 and 2). One heterozygous female had a likely seizure (only 2 recorded). The seizures occurred over days P14 to P20 with most occurring on days P17 and P18.

Supplementary material related to this article can be found online at

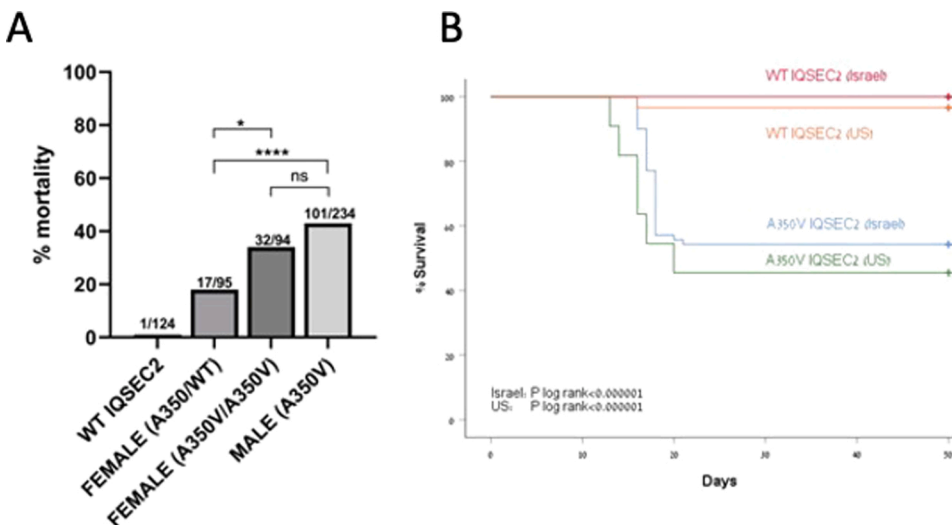


Fig. 1. Mortality associated with the A350V mutation in mice. (A) A highly significant difference in the mortality rate in the Technion facility was evaluated through 9 months of age between the 4 four groups ($p < 0.00001$ assessed by chi test). Specific pairwise comparisons showed significant differences between wild type and all other groups ($p < 0.00001$); heterozygote female vs homozygote female ($p = 0.011$); heterozygote female vs hemizygote male ($p = 0.000015$) * * * but not for homozygote female vs hemizygote male ($p = 0.128$) (NS). (B) Kaplan-Meier Survival Curve for wildtype (IQSEC2^{X/Y}) and mutant (IQSEC2^{A350V/Y}) male mice. Curves from Haifa Israel (Red/Blue) and Philadelphia USA (Orange/Green) are superimposed.

doi:10.1016/j.jhazmat.2021.126226.

To confirm that these events were electrographic seizures we video EEG recorded 20 pups ($n = 10$ WT males, 8 mutant males, and 2 heterozygous females) from P15 to P21 for 1–5 h a day. During the EEG recording, we captured 5 seizures in 3 mutant male animals. An example of a cluster of seizures in one male (Fig. 2A) and two additional seizures in two other mutant males (Fig. 2B and C). The seizures were a series of sharps that built in frequency during the movements (Fig. 2A inset). There were some events that on video we called seizure without clear EEG correlate, but with movement artifact making it difficult to determine if there was underlying electrographic changes. In addition to seizures, visually, the EEG of the hemizygous mutant male pups had sharps (Fig. 3C: *) that were recurrent and found in 6 out of 8 of the mutants but none of the wild type males (0 of 10).

The EEG from the pups was quantified by determining the frequency content of the recordings over the full 2–4 h of recordings (artifact rejected periods were not quantified). At all ages, the background activity in the delta band (0.5–3.5 Hz) was higher power between the wild type male and mutant male (Fig. 3D). This difference was only statistically significant at P16 and P19 (Two-way ANOVA genotype \times frequency: P16- $p = 0.0046$ [$F=4.69$]- multiple comparisons- $p = 0.0047$; P19- $p = 0.018$ [$F=3.18$]- multiple comparisons- $p = 0.037$). At P18, there was a difference between wildtype and mutant as a whole (P18-genotype \times frequency- $p = 0.018$), but no difference by multiple comparisons. The difference in the delta band appears to increase over time and then decrease at P20 (Fig. 3D, P20 graph; see Supplementary Fig. 1 for all ages). The lack of consistent statistical differences was likely due to numbers of animals recorded at each age.

For the mutant males and heterozygous and mutant females that survived past P21 and all littermate wildtype males and females we recorded for 72 h (between P30 and P90 with 4 recorded at P90) to look for seizures ($n = 9, 8, 8, 3$ respectively). No seizures were observed in any animal over this time period (30–90 days of age) during the 72 h of recording. Visually, the background EEG clearly had differences with spikes occurring in the mutant males in 8 of 9 animals and 0 of 9 wildtype males (Fig. 4B,C- C has isolated spikes from 2 mice). We next quantified the EEG in the adults as in the pups but using the full 72 h of EEG (Fig. 4D). The quantification was done for each electrode region (cortex and hippocampus) and for total time as well as dark and light times (Supplemental Fig. 2). There was a persistent difference in delta frequency band activity between the mutant males and wildtypes in the adult mice for hippocampal or cortex electrodes over the full 72 h (Two-way ANOVA genotype \times frequency: All-day- $p = 0.0048$ [$F=5.31$]-

multiple comparisons- $p = 0.0059$; All-Night- $p = 0.0223$ [$F=3.72$]- multiple comparisons- $p = 0.041$), but not in hippocampal or cortical electrodes separated (Supplementary Fig. 2).

3.3. RNAseq and analysis

We performed RNAseq as described in methods on 4 A350V male and 3 wild type male mice from the same litter at day 16. Heat maps of each of the mice are shown in Fig. 5a and volcano plot (Fig. 5b) showing the relative fold induction and directionality of change of the 431 differentially expressed genes (DEGs). Notable features of this RNAseq analysis include the absence of a change in the relative amount of IQSEC2 RNA between the WT and MT consistent with our previous observation that the A350V mutation has no effect on IQSEC2 protein levels. The most markedly induced gene in the entire data set was that for TRH (Thyrotropin Releasing Hormone) with an approximately 8-fold reduction in TRH RNA seen in d16 hippocampi of A350V mice. This finding for TRH was confirmed by qRT-PCR (TRH/HPRT 1.23 ± 0.23 in WT vs 0.16 ± 0.06 , $n = 6$ for both WT and MT mice; $p = 0.001$) as shown in Fig. 5c. The entire comparative dSeq analysis of all expressed genes in wild type and A350V mice is provided as an online supplement (Supplemental Table 1).

The 431 DEGs were analyzed by ingenuity pathway analysis software which allows for the identification of canonical biological pathways, networks and processes which are represented by clusters of these DEGs indicating a high probability that these pathways are disturbed by the A350V mutation at this time point in development. The most significantly affected pathway was that for synaptogenesis signaling which is consistent with the known anatomic location of IQSEC2 at the post synaptic density and its key function in mediating NMDA activity dependent changes in synaptic signaling (Shoubridge et al., 2010b; Myers et al., 2012; Brown et al., 2016). A complete list of other canonical pathways significantly overrepresented by these 431 DEGs is shown in Table 1. Furthermore, the most significantly associated neurological disease detected by the ingenuity pathway analysis was for epilepsy ($p = 7 \times 10^{-24}$), reflecting an association of 63 DEGs for this disease state.

4. Discussion

In this study we report several novel findings regarding epilepsy associated with an IQSEC2 mutation. We present here for the first time EEG based documentation of seizures in mice with a IQSEC2 mutation at young ages, but in mice that survive to adulthood, no seizures were observed. Second, we show marked abnormalities in delta waves that persist through adulthood consistent with our previous report of cognitive dysfunction in A350V mice even in mice without concurrent seizure activity. Finally, we present RNAseq data timed to be coincident with the onset of seizures and identify a significant dysfunction in multiple canonical signaling pathways that may serve as targets for therapy to prevent seizures.

Two independent groups have recently reported on murine knockout models of the IQSEC2 gene and possible seizure activity which appears to be different in its time of onset and associated mortality from that we have described here for the A350V missense mutation. Jackson and colleagues (Jackson et al., 2019) observed spontaneous seizure like activity by video and reported on the onset of seizures at day 16 in the male mice and continuing up to 4 months of age with an approximately overall 20% mortality rate in the male mice by 4 months of age. No EEGs were performed in this study. Sah and colleagues working with an independently derived IQSEC2 knockout model captured seizure like activity by video monitoring but failed to capture any epileptiform activity by EEG. Notably Sah and colleagues actually demonstrated decreased susceptibility to induced seizures in their knockout mice. The male knockout mice characterized by Sah and colleagues had a median lifespan of 95 days and 100% mortality by 6 months with the cause of

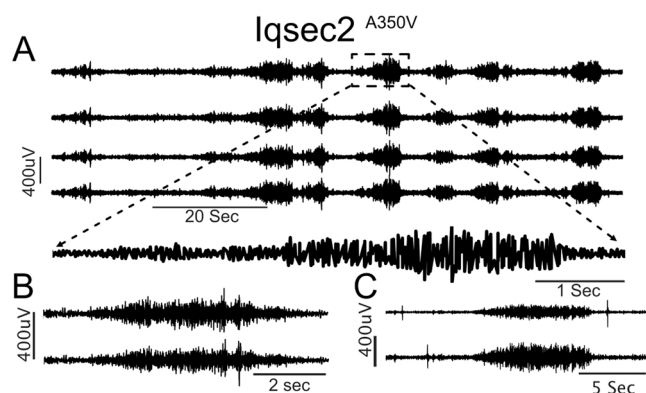


Fig. 2. Seizures in P15–P20 IQSEC2^{A350V/V} mutant mice. Three representative seizures are presented (Fig. 2A, B, C). (A) A prolonged time scale (scale bar 20 s) tracing demonstrating a cluster of brief seizures where the pup backs up, tail stiffens, and jumps up, with each run of spiking (see supplementary video 1 for example). Faster time scale of a brief seizure in 2 A is shown in the expanded inset. (B and C) Two other representative seizure examples are presented. Time scale per image. Voltage scale bar per image.

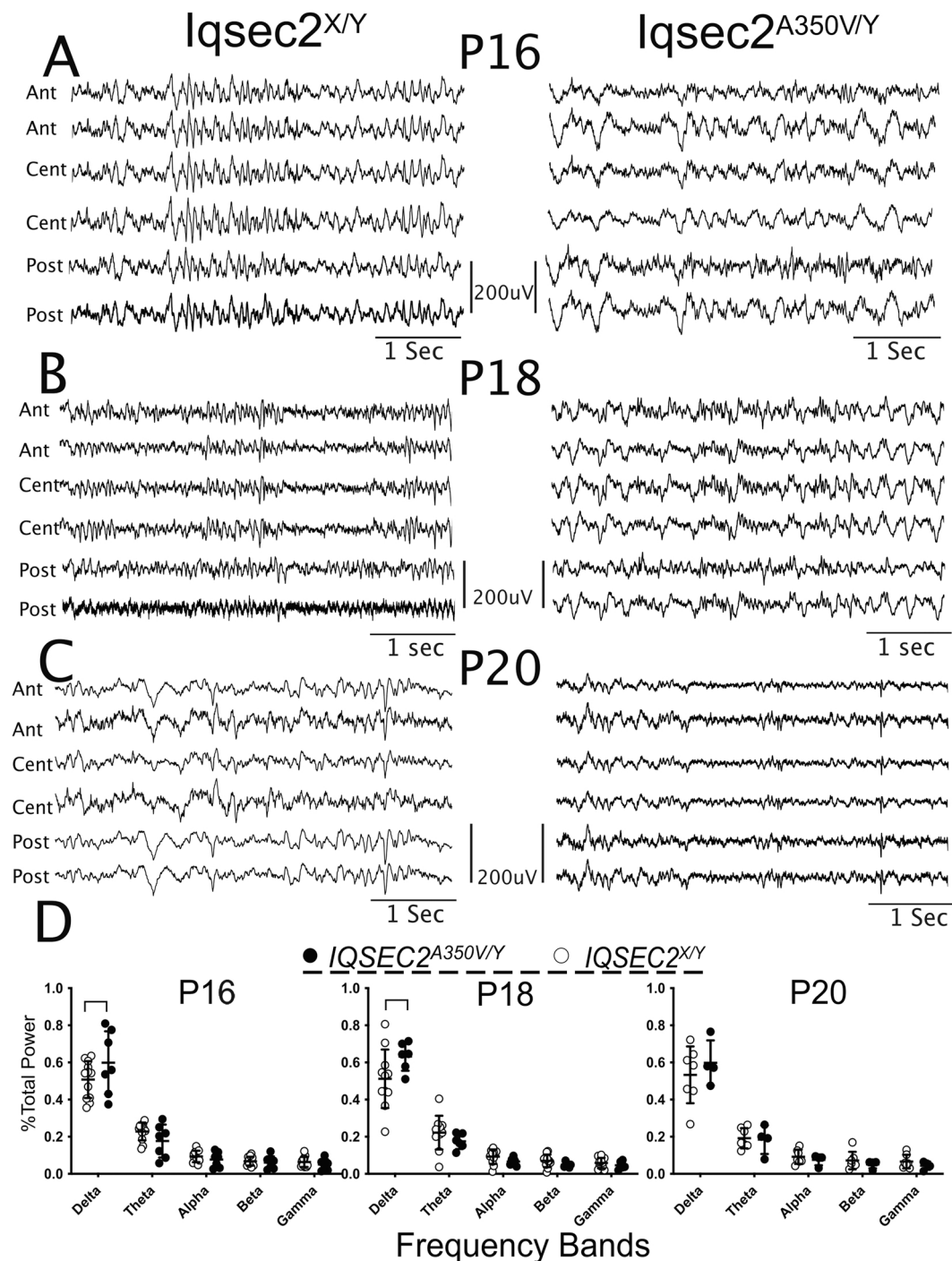


Fig. 3. Representative EEG and quantification from *IQSEC2*^{x/y} and *IQSEC2*^{A350V/Y} mice across the young age-span. (A) P16 (B) P18 and (C) P20 tracings from wildtype (left) and mutant (right) are shown. 6 of the 8 electrodes are presented. Spikes in the *IQSEC2*^{A350V/Y} mice are marked with *. (D) Representative plots of FFT power calculations at 3 ages (P16, P18, and P20). Power spectrum was broken up into EEG bands of Delta (0.5–3 Hz), Theta (3–8 Hz), Alpha (8–13 Hz), Beta (13–25 Hz), and Gamma (25–70 Hz). Statistically different bands are marked by *. See text for stats.

death presumed to be due to status epilepticus based on post mortem analysis of the mice found dead. We have found in the A350V mice a more defined seizure window of P16–20 with a 45% mortality rate during this period. That there exist differences between the *IQSEC2* knockout and A350V *IQSEC2* missense mutation models in seizure activity is not surprising. One possible explanation for differences in seizure activity between these models may be their different genetic backgrounds (C57Bl/6N-Hsd background for knockout of Jackson et al., 2019; C3HeB/FeJ x B6NJ for knockout of Sah et al.; C57Bl/6 J for

A350V model described in this study). A second likely contributor for the observed differences between the *IQSEC2* knockout and A350V *IQSEC2* missense mutation models in seizure activity is that the knockout is a total loss of *IQSEC2* function mutation while the A350V mutation appears to result in a constitutive activation of *IQSEC2* representing a gain of function mutation (Rogers et al., 2019). Changes in *IQSEC2* function would be expected to result in opposite effects on the amount of surface AMPA receptor in cells in which *IQSEC2* is expressed (Brown et al., 2016) with knockout mice having increased AMPAR

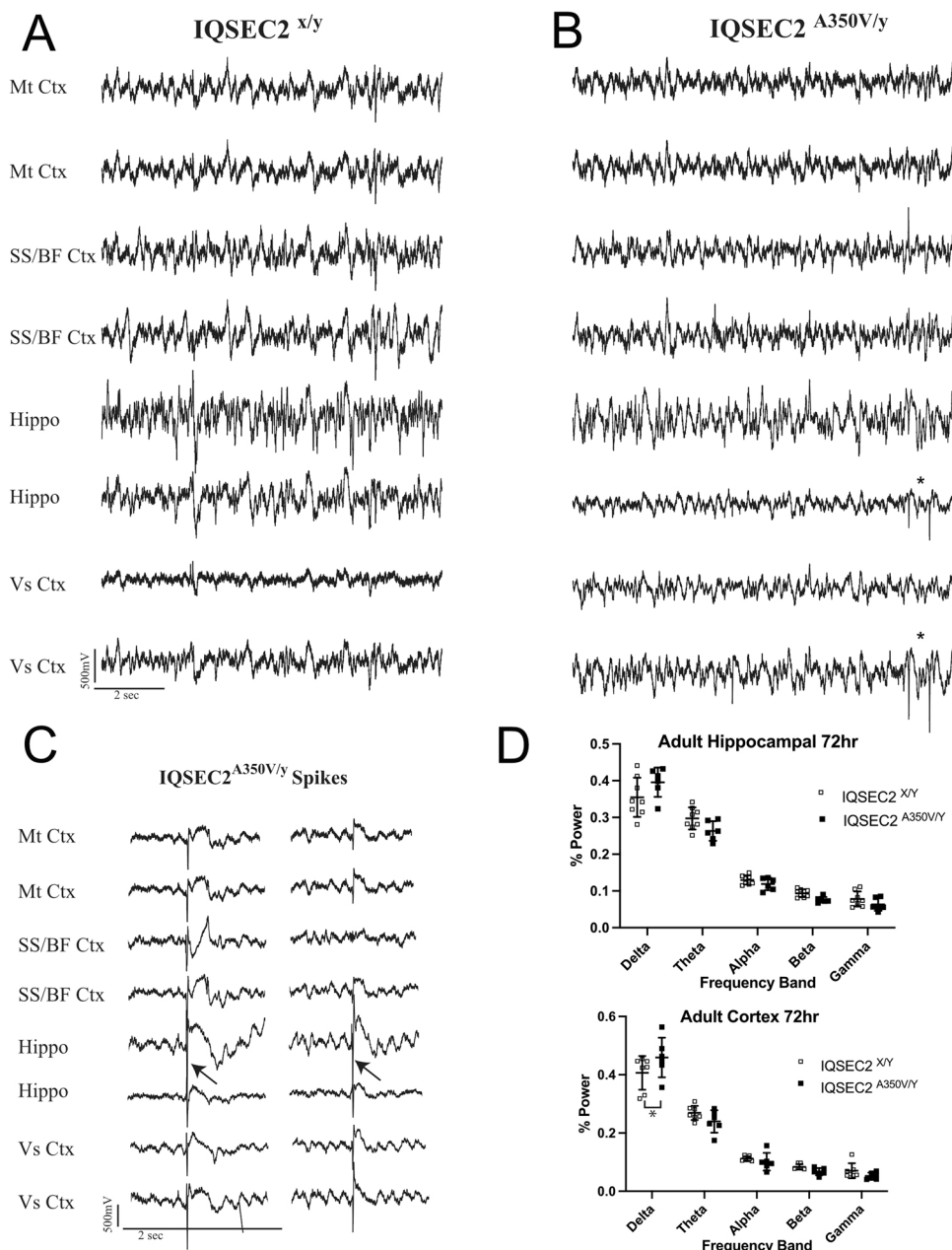


Fig. 4. Representative EEG and quantification from IQSEC2^{x/y} and IQSEC2^{A350V/y} adult mice. (A) wildtype tracings (B) mutant male tracing. In both representative mice the 8 implanted electrodes are shown. Spikes in the IQSEC2^{A350V/y} mice are marked with *. (C) Isolated spikes in the adult males are presented. 6 of 8 mutant males and no wildtype have these spikes. (D) Representative plots of FFT power calculations from hippocampal and cortical electrodes over the full 72hrs of recording is presented. Power spectrum was broken up into EEG bands of Delta (0.5–3 Hz), Theta (3–8 Hz), Alpha (8–13 Hz), Beta (13–25 Hz), and Gamma (25–70 Hz). Statistically different bands are marked by *. See text for stats.

surface expression while a gain of function mutation would result in decreased surface AMPAR expression. Consistent with this hypothesis in the Sah knockout model (Sah et al., 2020) the loss of function of IQSEC2 was associated with an increased number and excitatory drive onto parvalbumin GABAergic inhibitory interneurons which appeared to contribute to a hyperinhibited network. On the contrary, in the gain in function A350V model our hippocampal RNAseq data shows that parvalbumin mRNA expression is significantly decreased in A350V mice hippocampi (approximately 30% reduction, $p=0.006$; see dSeq results in supplemental file #1). Moreover, in hippocampal neurons differentiated from induced pluripotent stem cells derived from a patient with the A350V mutation, the percentage of GABAergic neurons was markedly decreased (Brant et al., 2021). The differences in the pattern of the seizures between different types of IQSEC2 mutations underscores the value of genotype specific models as platforms for drug discovery for prevention of seizures.

Our findings of change in the frequency content of the EEG in the mutant and wildtypes is consistent with many other developmental and

epileptic encephalopathy models (Marsh et al., 2009, Mulcahey et al., 2020 PMID). Interestingly, in some models there is a gain in delta power and others a loss. The A350V IQSEC2 model has a gain in delta which is consistent with the cognitive difference previously reported (Rogers et al., 2019). One aspect of this data is that the delta changes persisted in mice that we did not record having seizures as adults. This may be due to the fact that the mice were having seizures during early development but we could not track the mice for this study. This suggests that the network level changes induced by dysfunctional IQSEC2 may be at least partially unrelated to seizures and that simply stopping seizures in A350V mice may not completely prevent the development of cognitive impairment. Normalization of the background EEG could also be used as a outcome in any precision therapy.

The presence of spikes/sharps is consistent with the epilepsy phenotype that these mice develop. This also may suggest that while we only visually observed that 45% of the hemizygous males had seizures as pups, the frequency of seizures may have been higher and some pups having seizures may have survived. In the adult mutant mice, we did not

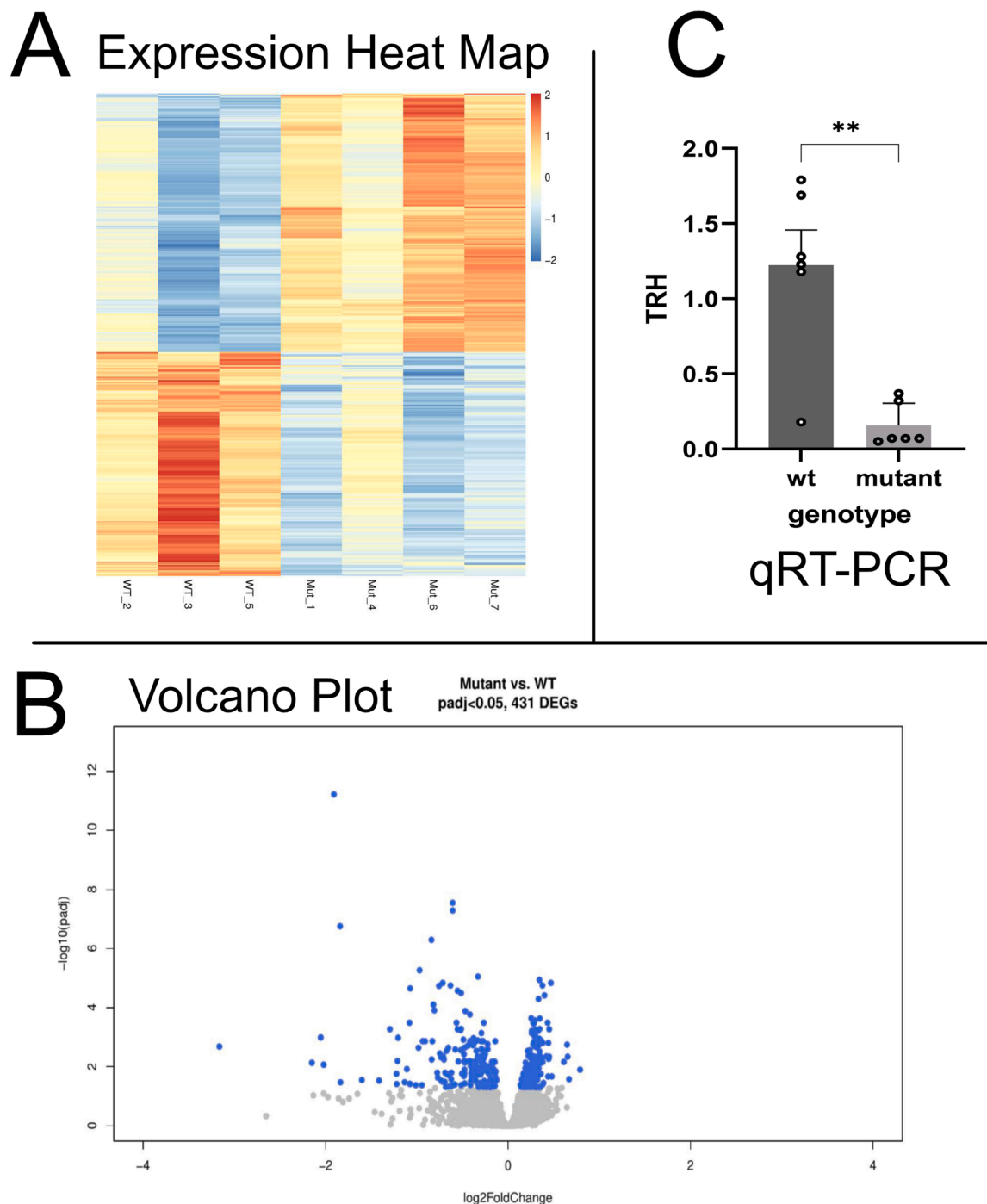


Fig. 5. RNAseq analysis of IQSEC2 Post natal day 16 cortices. (A) A Heat Map of relative expression of the 431 DEGs across all mice used to generate RNAseq data. Yellow orange indicating upregulation and blue indicating down regulation of the DEGs. (B) A Volcano Plot demonstrating the relative distribution of RNAseq data for the 431 DEGs (each DEG gene shown in purple) between A350V and wild type mice expressed as function of fold change and degree of significance. The cutoff for assigning a gene as being differentially expressed was a log padj of greater than 1.3 corresponding to a padj < 0.05. (C) TRH qRTPCR results in 6 MT and 6 WT mice. TRH mRNA was quantified by qRTPCR from 6 wild type and 6 A350V mice (MT) at day16 (TRH/HPRT 1.23 ± 0.24 in WT vs 0.16 ± 0.21 , $n = 6$ for both WT and MT mice; $**p = 0.001$).

observe seizures. This could represent a survivorship bias in the adult mice for those which are less susceptible to seizures or that they may have seizures, but infrequently, with a frequency of less than weekly. With our recording for 3 days in 9 mice, we would expect that we could detect a seizure frequency of at least weekly. More continuous recording using EEG or just video could be performed if a primary endpoint in a drug study was to measure change in seizure frequency. Alternatively, the presence of spiking could be used as an endpoint measure, though

whether an agent that could stop seizure could normalize the EEG is often not related.

The EEG and Seizure findings of the A350V Iqsec2 mouse now clearly models the DEEs with demonstration of the seizure phenotype in this mouse. The DEEs have an expanding genetic architecture (von Deimling et al., 2017) that includes a number of X-linked genes including *Arx*, *Cdkl5*, *Mecp2*, *Cask*, *Gabra3*, and others (Marsh et al., 2009; Tang et al., 2019; Niturad et al., 2017; Patel et al., 2020). All of these genes have

Table 1

IPA canonical pathways likely to be affected by the A350V IQSEC2 mutation based on DEGs.

Ingenuity Canonical Pathways	log (p-value)
Synaptogenesis Signaling Pathway	13.6
Calcium Signaling	12.1
Opioid Signaling Pathway	9.66
GABA Receptor Signaling	8.67
Endocannabinoid Neuronal Synapse Pathway	7.84
Synaptic Long Term Depression	7.07
Axonal Guidance Signaling	6.97
Netrin Signaling	6.54
CREB Signaling in Neurons	6.5
Neuropathic Pain Signaling In Dorsal Horn Neurons	6.46
Synaptic Long Term Potentiation	5.32
Epithelial Adherens Junction Signaling	5.31
Protein Kinase A Signaling	5.26
Rac Signaling	5.15
GNRH Signaling	4.7
Reelin Signaling in Neurons	4.57
RhoGDI Signaling	4.52
Corticotropin Releasing Hormone Signaling	4.1
Gap Junction Signaling	4.09
cAMP-mediated signaling	4.05
Ephrin Receptor Signaling	3.88
nNOS Signaling in Neurons	3.68
Signaling by Rho Family GTPases	3.2
Gαq Signaling	3.15
Actin Cytoskeleton Signaling	3.12
Gas Signaling	3.09
Ephrin A Signaling	2.78
Regulation of Actin-based Motility by Rho	2.76
Amyotrophic Lateral Sclerosis Signaling	2.68
Glutamate Receptor Signaling	2.41
RhoA Signaling	2.11
Neuroinflammation Signaling Pathway	2.01
Actin Nucleation by ARP-WASP Complex	1.98

epilepsy as a component phenotype, but *Mecp2* (cause of Rett Syndrome) and *Cask* mutations can have later onset and more variable epilepsy phenotype, as can IQSEC2 patients. The mouse models of these genes have variable seizure phenotypes with Arx mice recapitulating the human phenotype (Marsh et al., 2009), *Cask* and *Mecp2* having variable phenotypes and only in either female or male mice respectively (Patel et al., 2020; Wither et al., 2018), or in Cdkl5 mice there is a late onset seizure phenotype which is different then found in patients (Mulcahey et al., 2020). The A350V Iqsec2 mouse epilepsy fits within the models that fairly accurately recapitulate the human phenotype. Directly comparing this A350V model with the two other Iqsec2 mutation models demonstrates they all have seizures but the Shoubridge group (Jackson et al., 2019) reported a seizure phenotype but with variable penetrance, and the Frankel group (Sah et al., 2020) had lethal seizures but increased sensitivity to chemoconvulsants. Taken together, the A350V Iqsec2 mouse models are an X linked DEE, but with all of these models, there are interesting issues that if better understood could help understand the mouse and human phenotypes.

RNAseq analysis at P16, just prior to the onset of seizures, identified 431 DEGs. These DEGs were assessed using ingenuity pathway analysis software identifying several canonical pathways that were significantly affected by this A350V mutation. The most prominently affected pathway was that for synaptic signaling which is expected based on the known location of IQSEC2 at the post synaptic density and its role in mediating NMDA dependent changes of activity.

The most prominently dysregulated gene was that for TRH with an approximately 8-fold downregulation of TRH mRNA seen in the mutant mouse hippocampi. The TRH mRNA transcript codes for five copies of the mature TRH protein (a tripeptide) created by specific proteolytic cleavages of a single protein product. Furthermore, we found in our RNAseq analysis that the TRH degradation enzyme was significantly upregulated in the mutant hippocampus (25% upregulation,

$p < 0.0009$). The combined effect of the downregulation in TRH RNA (with each TRH mRNA molecule encoding 5 copies of TRH protein) and upregulation of its degradation pathway would suggest that the amount of TRH peptide would be decreased over 50 fold in the A350V IQSEC2 hippocampus compared to the wild type hippocampus. TRH has been demonstrated to have multiple neurotherapeutic effects independent from its endocrine actions with a distinct TRH receptor present in the hippocampus of both rodents and man (Kelly et al., 2015). Several clinical trials in man have demonstrated positive effects of TRH in many CNS disorders including drug resistant epilepsy suggesting that TRH or its more stable analogues might be used as therapy in A350V IQSEC2 mediated epileptic seizures (Kubek and Garg, 2002; Kubek et al., 2009; Takeuchi, 1996). JAK4D might be one such candidate based on its stability profile, selectivity for central TRH receptors and its ability to mimic the behavioral actions of TRH without evoking endocrine effects (Kelly et al., 2015).

Together, this work places the Iqsec2 A350V mouse in line with other DEE mouse lines that can be used to study the mechanisms and potential treatments of these disorders, and Iqsec2 related epilepsy specifically. The ascertainment of multiple dysregulated transcriptional pathways opens up possibilities of targeting the downstream effect of the Iqsec2 pathogenic variant and ultimately comparing this to the other Iqsec2 lines or mice with seizure onsets at the same developmental stage can yield novel opportunities for treatments.

Funding

None.

Acknowledgments

The authors wish to thank the Genomics Unit of the BCF unit of the Technion for their help in the RNAseq analysis and Mr. Paul Zino for expert care of the animal colony. This study was supported by NIH Grant NICHD 5U54HD086984-05.

Potential conflicts of interest

None.

Appendix A. Supporting information

Supplementary data associated with this article can be found in the online version at doi:10.1016/j.epilepsyres.2022.106907.

References

- Ahrens-Nicklas, R.C., Tecedor, L., Hall, A., Lysenko, E., Cohen, A.S., Davidson, B.L., Marsh, E.D., 2019. Neuronal network dysfunction precedes storage and neurodegeneration in a lysosomal storage disorder. *JCI Insight*.
- Brant, B., Stern, T., Shekhdem, H.A., Mizrahi, L., Rosh, I., Stern, Y., Ofer, P., Asleh, A., Umanah, G.K.E., Jada, R., Levy, N.S., Levy, A.P., Stern, S., 2021. IQSEC2 mutation associated with Epilepsy, Intellectual Disability and Autism results in Hyperexcitability of patient derived neurons and deficient synaptic transmission. *Molecular Psych.* 26 (12), 7498–7508. <https://doi.org/10.1038/s41380-021-01281-0>. Epub 2021 Sep 17. PMID: 34535765.
- Brown, J.C., Petersen, A., Zhong, L., Himelright, M.L., Murphy, J.A., Walikonis, R.S., Gerges, N.Z., 2016. Bidirectional regulation of synaptic transmission by BRAG1/IQSEC2 and its requirement in long-term depression. *Nat. Comm.* 7, 11080. <https://doi.org/10.1038/ncomms11080>.
- von Deimling, M., Helbig, I., Marsh, E.D., 2017. Epileptic encephalopathies-clinical syndromes and pathophysiological concepts. *Curr. Neurol. Neurosci. Rep.* 17 (2), 10.
- Hinze, S.J., Jackson, M.R., Lie, S., Jolly, L., Field, M., Barry, S.C., Harvey, R.J., Shoubridge, C., 2017. Incorrect dosage of IQSEC2, a known intellectual disability and epilepsy gene, disrupts dendritic spine morphogenesis. *Transl. Psych.* 7, e1110 <https://doi.org/10.1038/tp.2017.81>.
- Jackson, M.T., Loring, K.E., Homan, C.C., Thai, M.H.N., Maattanen, L., Arvio, M., Jarvela, I., Shaw, M., Gardner, A., Gecz, J., Shoubridge, C., 2019. Heterozygous loss of function of IQSEC2/Iqsec2 leads to increased activated Arf6 and severe neurocognitive seizure phenotype in females. *Life Sci. Alliance* 2, e201900386.
- Kelly, J.A., Boyle, N.T., Cole, N., Slatore, G.R., Colivicchi, M.A., Stefanni, C., Gobbo, O.L., Scalabrino, G.A., Ryan, S.M., Elamin, M., Walsh, C., Vajda, A., Goggin, M.M.,

- Campbell, M., Mash, D.C., OMara, S.M., Brayden, D.J., Callanan, J.J., Tipton, K.F., Della Corte, L., Hunter, J., O'Boyle, K.M., Williams, C.H., Hardiman, O., 2015. First in class thyrotropin releasing hormone (TRH) based compound binds to a pharmacologically distinct TRH receptor subtype in human brain and is effective in neurodegenerative models. *Neuropharmacology* 89, 193–203.
- Kubek, M.J., Garg, B.P., 2002. Thyrotropin releasing hormone in the treatment of intractable epilepsy. *Pediatr. Neurol.* 26, 9–17.
- Kubek, M.J., Domb, A.J., Veonesi, M.C., 2009. Attenuation of kindled seizures by intranasal delivery of neuropeptide loaded nanoparticles. *Neurotherapeutics* 2, 359–371.
- Levy, N.S., Umanah, G.K.E., Rogers, E.J., Jada, R., Lache, O., Levy, A.P., 2019. IQSEC2 associated intellectual disability and autism. *Int. J. Mol. Sci.* 20 <https://doi.org/10.3390/ijms20123038>.
- Marsh, E., Fulp, C., Gomez, E., Nasrallah, I., Minarcik, J., Sudi, J., Christian, S.L., Mancini, G., Labosky, P., Dobyns, W., Brooks-Kayal, A., Golden, J.A., 2009. Targeted loss of Arx results in a developmental epilepsy mouse model and recapitulates the human phenotype in heterozygous females. *Brain* 132, 1563–1576.
- Michalakakis, M., Holsinger, D., Ikeda-Douglas, C., Cammisuli, S., Ferbinteanu, J., DeSouza, C., DeSouza, S., Fecteau, J., Racine, R.J., Milgram, N.W., 1998. Development of spontaneous seizures over extended electrical kindling. I. Electrographic, behavioral, and transfer kindling correlates. *Brain Res.* 793, 197–211.
- Mignot, C., Depienne, C., 2019. IQSEC2 related encephalopathy in males and females: a comparative study including 37 novel patients. *Genet. Med.* 21, 837–849.
- Mulcahey, P.J., Tang, S., Takano, H., White, A., Davila Portillo, D.R., Kane, O.M., Marsh, E.D., Zhou, Z., Coulter, D.A., 2020. Aged heterozygous Cdkl5 mutant mice exhibit spontaneous epileptic spasms. *Exp. Neurol.* Oct. 332, 113388.
- Murphy, J.A., Jense, O.N., Walikonis, R.S., 2006. BRAG1 a Sec7 domain containing protein is a component of the postsynaptic density of excitatory synapses. *Brain Res.* 2006 (1120), 35–45.
- Myers, K.R., Wang, G., Sheng, Y., Conger, K.K., Casanova, J.E., Zhu, J.J., 2012. Arf6-GEF BRAG1 regulates JNK-mediated synaptic removal of GluA1-containing AMPA receptors: a new mechanism for nonsyndromic X-linked mental disorder. *J. Neurosci.* 32, 11716–11726.
- Niturd, C.E., Lev, D., Kalscheuer, V.M., et al., 2017. Rare GABRA3 variants are associated with epileptic seizures, encephalopathy and dysmorphic features. *Brain* 140 (11), 2879–2894. Nov 1.
- Patel, P.A., Liang, C., Arora, A., Vijayan, S., Ahuja, S., Wagley, P.K., Settlege, R., LaConte, L.E.W., Goodkin, H.P., Lazar, I., Srivastava, S., Mukherjee, K., 2020. Haploinsufficiency of X-linked intellectual disability gene CASK induces post-transcriptional changes in synaptic and cellular metabolic pathways. *Exp. Neurol.* Jul. 329, 113319.
- Raol, Y.H., Lapidus, D.A., Keating, J.G., Brooks-Kayal, A.R., Cooper, E.C., 2009. A KCNQ channel opener for experimental neonatal seizures and status epilepticus. *Ann. Neurol.* 65, 326–336.
- Rogers, E.J., Jada, R., Schagenheim-Rozales, K., Sah, M., Cortes, M., Florence, M., Levy, N.S., Moss, R., Walkonis, R.S., Gerges, N.Z., Kahn, I., Umanah, G.K.E., Levy, A.P., 2019. An IQSEC2 mutation associated with intellectual disability and autism results in decreased surface AMPA receptors. *Front. Mol. Neurosci.* 12, 43. <https://doi.org/10.3389/fnmol.2019.00043>.
- Sah, M., Shore, A.N., Petri, S., Kanber, A., Yang, M., Weston, M.C., Frankel, W.N., 2020. Altered excitatory transmission onto hippocampal interneurons in the IQSEC2 mouse model of X linked neurodevelopmental disease. *Neurobiol. Dis.* 137, 104758, 2020.
- Sakagami, H., Sanda, M., Fukaya, M., Miyazaki, T., Sukegawa, J., Yanagisawa, T., Miyazaki, T., Sukegawa, J., Yanagisawa, T., Suzuki, T., Fukunaga, K., Watanabe, M., Kondo, H., 2008. IQ-ArfGEF/BRAG1 is a guanine nucleotide exchange factor for ARF6 that interacts with PSD-95 at post-synaptic density of excitatory synapses. *Neuro Res.* 60, 199–212. <https://doi.org/10.1016/j.neures.2007.10.013>.
- Scantlebury, M.H., Galanopoulou, A.S., Chudomelova, L., Raffo, E., Betancourt, D., Moshé, S.L., 2010. A model of symptomatic infantile spasms syndrome. *Neurobiol. Dis.* 37, 604–612.
- Shoubridge, C., Tarpey, P.S., Abidi, F., Ramsden, S.L., Rujirabenjerd, S., Murphy, J.A., Boyle, J., Shaw, M., Gardner, A., Proos, A., Puusepp, H., Raymond, F.L., Schwartz, C. E., Stevenson, R.E., Turner, G., Field, M., Walikonis, R.S., Harvey, R.J., Hackett, A., Futreal, P.A., Stratton, M.R., Geck, J., 2010. Mutations in the guanine nucleotide exchange factor gene IQSEC2 cause nonsyndromic intellectual disability. *Nat. Genet.* 42, 486–488. <https://doi.org/10.1038/ng.588>.
- Shoubridge, C., Harvey, R.J., Dudding-Byth, T., 2019. IQSEC2 mutation update and review of the female-specific phenotype spectrum including intellectual disability and epilepsy. *Hum. Mutat.* 40, 5–24.
- Takeuchi, Y., 1996. Thyrotropin releasing hormone. Role in the treatment of epilepsy. *CNS Drugs* 6, 341–350.
- Tang, S., Terzic, B., Wang, L.J., et al., 2019. Altered NMDAR signaling underlies autistic-like features in mouse models of CDKL5 deficiency disorder. *Nat. Commun.* 10 (1), 2655. Jun 14.
- Wither, R.G., Colic, S., Bardakjian, B.L., Snead 3rd, O.C., Zhang, L., Eubanks, J.H., 2018. Electrographic and pharmacological characterization of a progressive epilepsy phenotype in female *MeCP2*-deficient mice. *Epilepsy Res.* 140, 177–183.
- Zerem, A., Haginoya, K., Lev, D., Blumkin, L., Kivity, S., Linder, I., Shoubridge, C., Palmer, E.E., Field, M., Boyle, J., Chitayat, D., Gaillard, W.D., Kossoff, E.H., Willems, M., Genevieve, D., Tran-Mau-Them, F., Epstein, O., Heyman, E., Dugan, S., Masurel-Paulet, A., Piton, A., Kleefstra, T., Pfundt, R., Sato, R., Tzschach, A., Matusmoto, N., Saitsu, H., Leshinsky-Silver, E., Lerman-Sagie, T., 2016. The molecular and phenotypic spectrum of IQSEC2-related epilepsy. *Epilepsia* 57, 1858–1869. <https://doi.org/10.1111/epi.13560>.
- Zipper, R., Baine, S.D., Genizi, J., Maoz, H., Levy, N.S., Levy, A.P., 2017. Developmental progression of intellectual disability, autism and epilepsy in a child with an IQSEC2 gene mutation. *Clin. Case Rep.* 5, 1639–1643. <https://doi.org/10.1002/ccr3.1139>.